Physically Based Equation for Phase Composition Curve of Frozen Soils

Zhen Liu and Xiong (Bill) Yu

The relationship between unfrozen water content (or saturation in freezing and thawing) and temperature, which is referred to as the phase composition curve in frozen soils, is a fundamental relationship in cold regions engineering. Because of the lack of a physical basis, there have been only empirical equations for this relationship. This study investigated the mechanisms underlying the phase composition curve. A detailed physical basis was established on the basis of the soil freezing characteristic curve, the Clapeyron equation, and the bundle of cylindrical capillary model. From this physical basis, a closed-form equation was developed for the formulation and prediction of this curve. This physically based equation quantifies the unique correlation between saturation and temperature in frozen soils and takes various factors into account, such as the soil saturation under unfrozen conditions and the lowest temperature used in experiments. The equation was validated with phase composition data measured with a thermal–time domain reflectometry sensor. In addition, the flexibility of the equation and its excellent applicability in various soils with a wide range of properties, in large temperature ranges, and in both freezing and thawing processes (hysteresis) were proved with reported data.

It has long been observed that there exists a relationship between unfrozen water content and temperature in frozen soils (*1–3*). For example, a considerable amount of data was published in the Proceedings of the First International Permafrost Conference, in 1966 (*4*). The curve for this relationship is frequently referred to as the phase composition curve in frozen soils. It is recognized as a fundamental relationship in cold regions engineering (*5*) because this curve offers a constitutive relationship between two fundamental quantities in frozen soils—unfrozen water content and temperature—and thus links the phase change of water to temperature. The relationship also casts light on other important parameters in cold regions engineering practice, such as the segregation potential for frost heave (*6*).

Empirical equations have usually been used to formulate the phase composition curve. Anderson and Tice found that the unfrozen water content of most frozen soils can be conveniently expressed as a function of temperature by a simple power curve (*3*):

$$\theta_w = C_1 (T_0 - T)^{C_2} \qquad (1)$$

Z. Liu, Bingham 256, and X. Yu, Bingham 206, Department of Civil Engineering, Case Western Reserve University, 2104 Adelbert Road, Cleveland, OH 44106-7201. Corresponding author: X. Yu, xxy21@case.edu.

where

θ_w = volumetric water content,
C_i = fitting constants indexed by i,
T_0 = freezing temperature of bulk water, and
T = temperature.

Alternatively, the gravimetric water content can be used. In this study the volumetric water content is adopted to facilitate the later theory presentations. Dillon and Andersland proposed a prediction equation by incorporating the specific surface area, the Atterberg limits, temperature, clay mineral type, and a defined activity ratio for soils (*7*):

$$\theta_w = \frac{2.8 \times 10^{-7} \rho_d s}{\rho_w A} \frac{T}{T_0} \qquad (2)$$

where

ρ_d, ρ_w = soil dry density and water density, respectively;
s = specific surface area; and
A = ratio between plastic index and percentage of soil grains less than 2 μm.

Equation 2 yielded good agreement when tested against 11 soils. But this equation was shown to be incapable of fitting complete phase composition curves, especially at higher temperatures (*4*). Similarly, Anderson and Tice suggested an equation based on a regression analysis of phase composition data for various soils (*3*). This equation predicts that water content is a function of the specific surface area and temperature:

$$\theta_w = C_1 + s^{C_2} + (T - T_0)^{C_3 s^{C_4}} \qquad (3)$$

The preceding equations are of an empirical nature and thus it is hard to guarantee satisfactory predictions under various conditions. The fact that only empirical equations are available is possibly due to unrevealed physical mechanisms underlying the phase composition curve. Both the lack of a reliable prediction equation and the absence of a solid physical background have been impeding more extensive applications of this relationship. In order to address this knowledge gap, this study presents a physical description for the phase composition curve in frozen soils. On the basis of the description, a closed-form equation for this relationship is proposed. The excellent performance and wide applicability of the physically based equation are demonstrated.

PHYSICAL MECHANISMS UNDERLYING PHASE COMPOSITION CURVE

The existence of the phase composition curve is attributed to two physical mechanisms. The first mechanism is the soil freezing characteristic curve (*2, 8, 9*), which establishes a relationship between
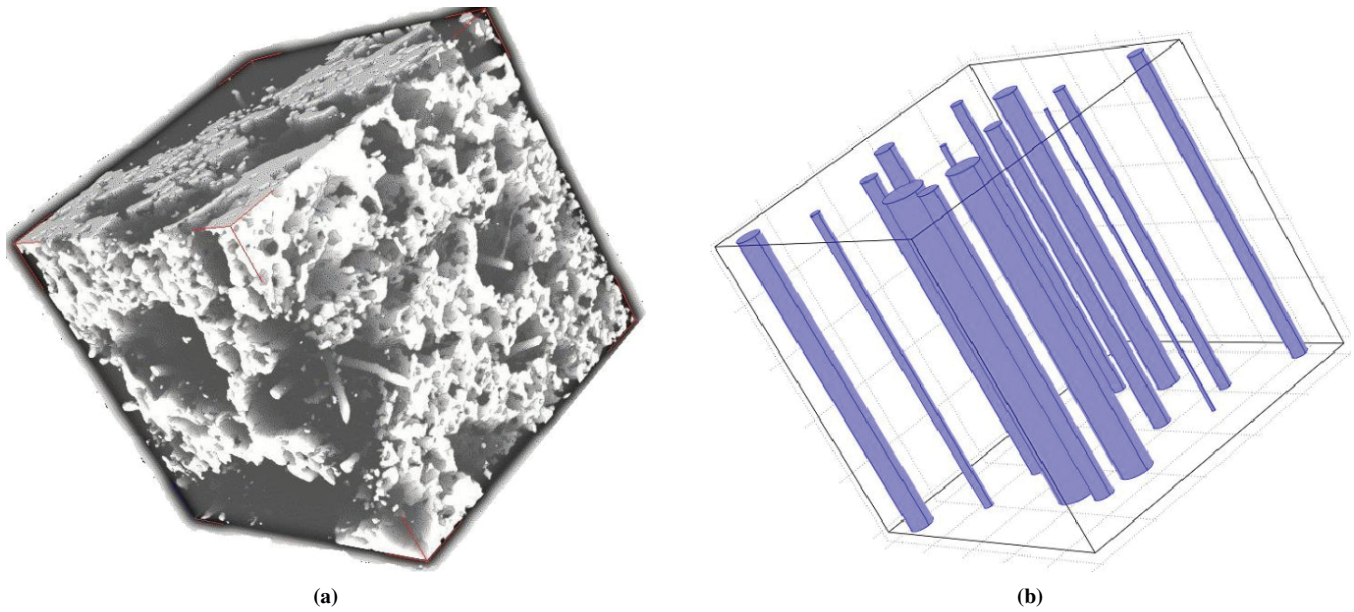
(a)

(b)

FIGURE 1   Internal structure of soil and its conceptualization: (*a*) computer tomography of soil sample and (*b*) element of BCC model.

the suction and unfrozen water content in frozen soils. This relation can be expressed as follows:

$$\psi = \psi(S) \tag{4}$$

where ψ is the soil suction and S is the saturation. S is equivalent to the unfrozen water content in a freezing-and-thawing process. This concept will be used throughout. The soil freezing characteristic curve describes the relationship between the system energy and the unfrozen water content in a frozen soil. Because of the similarity between the freezing-and-thawing process and the drying-and-wetting process, the soil freezing characteristic curve resembles the soil water characteristic curve in many ways (*2, 8*). So the bundle of cylindrical capillary (BCC) model, in which a soil is conceptualized as a bundle of cylindrical capillaries, can be extended from partially saturated soils to partially frozen soils (*10*). As can be seen in Figure 1*a*, a soil, as a typical porous medium, consists of a porous structure with pores at various scales. According to the BCC model, a soil with the morphology shown in Figure 1*a* can be equivalently converted into a conceptualized soil as shown in Figure 1*b*.

The purpose of introducing this conceptual model is to offer a feasible way to describe the pressure equilibrium in the process of ice formation. Pressures of water and ice within a pore are therefore connected to the pore morphology by the Young–Laplace equation:

$$\Delta p = \gamma \nabla \cdot \mathbf{n} = \gamma \left(\frac{1}{r_1} + \frac{1}{r_2} \right) \tag{5}$$

where

Δp = pressure difference across water–ice interface (meniscus, Figure 2),
γ = surface tension on interface,
$\mathbf{n}$ = unit outward normal vector of water–ice interface, and
r_1, r_2 = principal diameters of two-dimensional interface.

If Equation 5 is applied to cylindrical capillaries, the following equation is obtained:

$$p_\alpha - p_\beta = \frac{2\gamma \cos\phi}{r} \tag{6}$$

where

p_α, p_β = internal and external pressures of spherical surface,
r = its radius, and
ϕ = contact angle.

In an unsaturated soil, for example, its internal structure can be conceptualized as a two-dimensional BCC model as shown by Figure 2. For each capillary, there exists a meniscus between water and ice or between water and air. The matric suction for partially frozen (partially saturated) conditions is calculated as follows:

$$\psi = p_w - p_i \qquad (\psi = p_w - p_a) \tag{7}$$

where

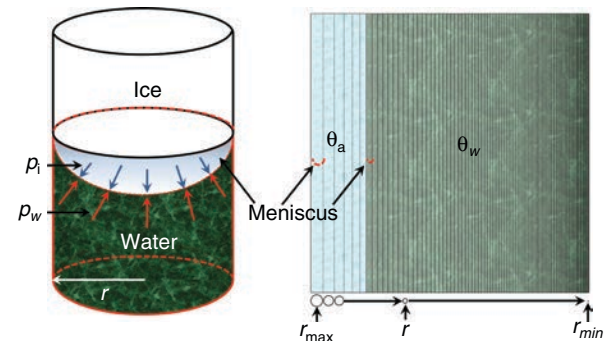p_w = water,
p_i = ice, and
p_a = air pressure.

FIGURE 2   BCC model for soils (max = maximum; min = minimum.

When the osmotic pressure caused by the chemical potential of solvents in saline conditions is neglected, soil suction is equal to matric suction. Thus suction in any cylindrical capillary when freezing (wetting) can be calculated as follows:

$$\psi = \frac{2\gamma_{wi}\cos\phi}{r} \qquad \left(\psi = \frac{2\gamma_{wa}\cos\phi}{r}\right) \tag{8}$$

As shown in Figure 2, two particular suction conditions can be obtained based on the foregoing introduction (*11*):

$$\psi_{max} = \frac{2\gamma_{wa}\cos\phi}{r_{min}} \tag{9}$$

$$\psi_{min} = \frac{2\gamma_{wi}\cos\phi}{r_{max}} \tag{10}$$

Therefore, the maximum matric suction, ψ_{min}, corresponds to the minimum pore radius r_{min} and the air-entry suction, ψ_{min}, corresponds to the maximum pore radius r_{max}.

In frozen soils, the second mechanism needs be to recalled before the first one has finished being introduced. The second mechanism is the Clapeyron equation, which predicts that the freezing point of water will decrease to somewhat below the freezing point of bulk water because of the presence of suction.

$$T = T_0 \exp\left(\frac{\psi}{-\rho_w L}\right) \tag{11}$$

where ρ_w is the water density and L is the latent heat of water fusion. Equation 11 was obtained on the basis of the original equation (*12, 13*) by assuming that the ice pressure is zero; this assumption is more a rule than an exception when ice lenses are absent. Another assumption is that the freezing or drying process is comparatively slow so that the thermodynamic equilibrium can be ensured on the water–ice interface.

According to Equations 8 and 11, ice formation occurs in larger pores first, which correspond to higher temperatures (freezing point). As shown in Figure 3, ice formation starts in the pore with the largest radius, r_{max}, if the sample is saturated with water. But if it is an unsaturated soil with saturation S_H under unfrozen conditions, ice formation starts at a temperature T_H, which represents the highest temperature at which ice can form. As freezing develops, more volume originally occupied by water is taken by ice. That is, saturation will decrease to zero as water in the smallest pores turns to ice; this process requires a temperature much lower than the freezing point of bulk water. For most experiments for the phase composition curve, the lowest tem-

perature that can be achieved, T_L, is much higher than the temperature corresponding to zero saturation. Accordingly, S_L is the lowest saturation that can be reached. So the temperature in any experiment for the phase composition curve should satisfy the following relationship:

$$\text{absolute zero} < T_L < T < T_H < T_{max} < T_0 \tag{12}$$

To return to the formation of the soil freezing characteristic curve, from the preceding introduction, saturation can be integrated from the pore volumes by the following equation (*14*):

$$S(r) = \int_{r_{min}}^{r} f(x)V(x)dx \tag{13}$$

where $f(r)$ is the probability density pore corresponding to radius r and $V(r)$ is the volume occupied by a single pore of radius r (*11*). It is therefore not difficult to infer that the saturated volumetric water content is reached in the largest pore:

$$S(r_{max}) = 1 \tag{14}$$

By the combination of the foregoing equations, the freezing water characteristic can be obtained with pore-size distribution and contact angle as follows (*11*):

$$S(\psi) = \int_{\psi_{max}}^{\psi} f\left(\frac{2\gamma_{wi}\cos\phi}{y}\right)V(y)d\left(\frac{2\gamma_{wi}\cos\phi}{y}\right)$$

$$= \int_{\psi}^{\psi_{max}} f\left(\frac{2\gamma_{wi}\cos\phi}{y}\right)V(y)\frac{2\gamma_{wi}\cos\phi}{y^2}d(y) \tag{15}$$

where y used in the integration is a dummy variable representing suction. Corresponding to temperature, the saturation measured in the freezing process of an unsaturated soil should satisfy

$$0 < S_L < S < S_H < 1 \tag{16}$$

On the basis of Equations 4 and 15, the unique relationship between saturation and temperature can be determined. The mathematical expression is introduced in the next section.

PHYSICALLY BASED PREDICTION EQUATION

A prediction equation can be obtained based on the physical mechanisms introduced in the last section. Aside from the formation of the soil freezing characteristic curve, various functions have been
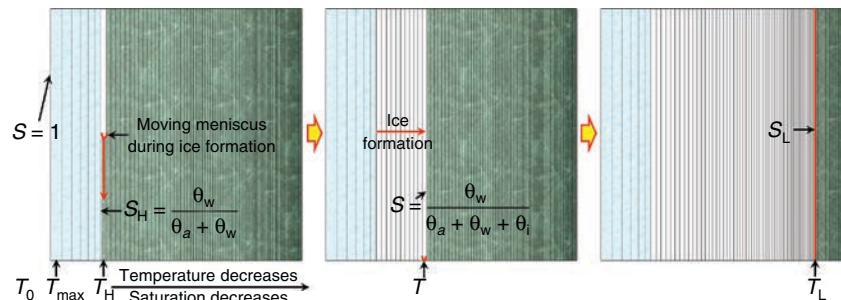

FIGURE 3   Freezing process in BCC model.

proposed for the soil water characteristic curve. In view of the similarity between the freezing and drying processes, these equations can also be taken for the prediction of the soil freezing characteristic curve. The following one was suggested by van Genuchten (15):

$$S = \left[\frac{1}{1+(\alpha\psi)^n}\right]^m \tag{17}$$

where α, m, and n are fitting constants, and S is the saturation in the freezing–thawing process, that is, the ratio of the volumetric unfrozen water content to the porosity (total volume ratio of unfrozen and frozen water). Equation 17 is reformulated as

$$\psi = \frac{1}{\alpha}\left(1 - S^{-1/m}\right)^{1/n} \tag{18}$$

Substituting Equation 18 into Equation 11, one obtains

$$T = T(S) = T_0 \exp\left[-\frac{1}{\alpha\rho_w L}\left(S^{-1/m} - 1\right)^{1/n}\right] \tag{19}$$

Equation 19 predicts the relationship between temperature and saturation in frozen soils that are either saturated or unsaturated under unfrozen conditions. But further considerations are necessary for applying this equation to the curve fitting of measured phase composition curves because, as mentioned earlier, the temperature for zero saturation in phase composition curves usually cannot be achieved by most experiments. In fact, a temperature that is several kelvins below the freezing point of bulk water is usually used as the lowest temperature. However, most experiments assume that all of the water has turned into ice at this lowest temperature. This assumption makes the measured saturation different from the true saturation used in Equation 19. In addition, the unsaturated condition under unfrozen conditions needs to be taken into account because in many cases saturation is measured with reference to the water content under frozen conditions. Even if a fully saturated specimen is claimed to be used, the slightly unsaturated condition will also result in a difference between the measured and the true saturation. From these concerns, the measured saturation in the phase composition curve can be related to the true saturation as follows:

$$S_M = \frac{S - S_L}{S_H - S_L} \tag{20}$$

where S_M and S are the measured saturation and true saturation, respectively. Hence the true saturation can be expressed by the measured value as follows:

$$S = S_M S_H - S_M S_L + S_L \tag{21}$$

Substituting Equation 21 into Equation 19 yields the prediction equation for the phase composition curve. Equation 12 can be used directly to fit the measured data.

$$T(S) = 273.15 \exp\left\{-\frac{1}{3.34 \times 10^8 \alpha}\left[\left(S_M S_H - S_M \theta_L + \theta_L\right)^{-1/m} - 1\right]^{1/n}\right\} \tag{22}$$

where

$T_0 = 273.15$ K,
$L = 3.34 \times 10^5$ J/kg, and
$\rho_w = 1{,}000$ kg/m³.

It can be seen that Equation 22 describes the unique relationship between saturation and temperature. Additional parameters, such as the specific area used in previous studies (Equations 2 and 3), are no longer necessary.

One advantage of Equation 22 is that it can be used to fit measured relationships between temperature and saturation when the saturation of the soil under unfrozen conditions is unknown. Also, the water content can be either volumetric or gravimetric. The fitting results will indicate whether the soil specimen is saturated by water before freezing occurs and indicate this water saturation. The second advantage is that the whole range of the phase composition curve can be reproduced by using measured data at a relatively small temperature range. Therefore, the experimental efforts in achieving extremely low temperature and ensuring precise experimental controls can be saved. As a result, any portion of a measured curve can be fitted by using Equation 22. And the unit of the water content (gravimetric or volumetric) does not cause extra difficulties in the fitting process. That is, the fitting function is able to predict the whole range of the phase composition curve based on the information carried by the available portion. However, under this condition, the calculated S_H and S_L represent the highest and lowest saturations of the data range, respectively, which are different from the physical meanings mentioned earlier.

APPLICATION OF EQUATION AND EXPERIMENTAL VALIDATION

A thermo–time domain reflectometry (TDR) sensor was used by the authors to measure the phase composition curves of two soils in a previous study (9). The thermo–TDR sensor is a combination of thermocouples and a conventional TDR sensor. Thus temperature and water content can be monitored simultaneously with the sensor. Temperature can be related to suction by ensuring the thermodynamic equilibrium on the water–ice interface with a relatively slow freezing–thawing rate, and unfrozen water content can be calculated by using water content at different degrees of freezing and thawing. Therefore, phase composition curves can be measured with this thermo–TDR sensor. More details about the theoretical background and sensor design for applying the thermo–TDR sensor to the measurement of phase composition curves can be found in the previous study (9). Thus only the necessary information for materials and specimen preparation is provided here for a better understanding.

Experiments were conducted on two representative types of subgrade soils in the state of Ohio. The index properties of these soils are summarized in Table 1. Soil specimens with a high water content (nearly saturated) were prepared and the thermo–TDR probes were installed in the soil specimens. The specimens and sensor were sealed with plastic wrap to prevent evaporation and then placed in a freezer at $-18°C$ (255 K) for approximately 24 h to be completely frozen. Thawing was initiated by cutting the power to the freezer, and monitoring of the TDR and temperature data was started at the same time until the specimen completely thawed.

For Soil 1, specimens were prepared by using a Harvard miniature compactor. The method of compaction—that is, the mass of soil solids in each layer and amount of compaction energy—was carefully controlled to ensure that the specimens were uniform. The specimens were 71 mm in height and 35 mm in diameter. Three probes were inserted mechanically to full depth along the axis of the cylindrical soil specimens with the middle probe directly on the axis.

TABLE 1 Index Properties of Soils Tested in This Study

Soil	Gravel	Coarse Sand	Fine Sand	Silt	Clay	Liquid Limit	Plastic Limit	Plastic Index
1	7	5	10	28	50	25	14	11
2	10	7	10	14	59	40	18	22

Specimens made of Soil 2 were prepared in a different way to determine if different geometries would affect the results. A steel ring with an inner diameter of 71 mm and a height of 200 mm was used, and 100 g of soil was placed in the ring on a steel table. The upper surface of the soil mass was flattened and then hammered for 12 blows with a 5-kg steel cylinder with a diameter of 71 mm dropped from a height of 200 mm.

The molded soil specimens were cylinders with a diameter of 71 mm and a height of about 12 mm. Because of the small height of the soil specimens, the thermo–TDR was inserted into the specimen with the probes perpendicular to the axis of the cylinder and the middle probe intersecting the axis. For each soil, duplicate specimens were made, from which one specimen was used for the thawing test and the others were reserved for results validation with the filter paper method. For both specimens made of Soil 1 and Soil 2, the thawing processes took more than 10 h. Accordingly, the rate of thermal exchange was smaller than 20 W/m^2 during the thawing process, which was experimentally proved to be enough to ensure the quasi-state of thermodynamic equilibrium.

Shown in Figure 4 are the comparisons between the measured and fitted phase composition curves for the two soils. The validity of the measured phase composition curves was proved by Liu et al. (9). All of the curve fitting was conducted with the data analysis package Origin. For both soils, the proposed prediction equation offered very good predictions in the whole range of the measured data. For the specimen made of Soil 1, there is still a considerable amount of unfrozen water (10%) in the frozen soils at 255 K, whereas for Soil 2, nearly 20% of the water still exists in the liquid form at 260 K. This finding proves that consideration of the saturation at the lowest temperature of an experiment is necessary. The water saturation under unfrozen conditions was estimated to be 100% and 97.91% for the specimens made of Soil 1 and Soil 2, respectively. This finding indicates that good saturation was obtained for both specimens. The value of S_H for Soil 1 violates the constraint set by Equation 16. But it is acceptable because the curve fitting is based on measured data with the damped least-squares algorithm. The result can be improved with better measured data. The excellent agreement between measured and fitted results proved the effectiveness of the proposed equation.
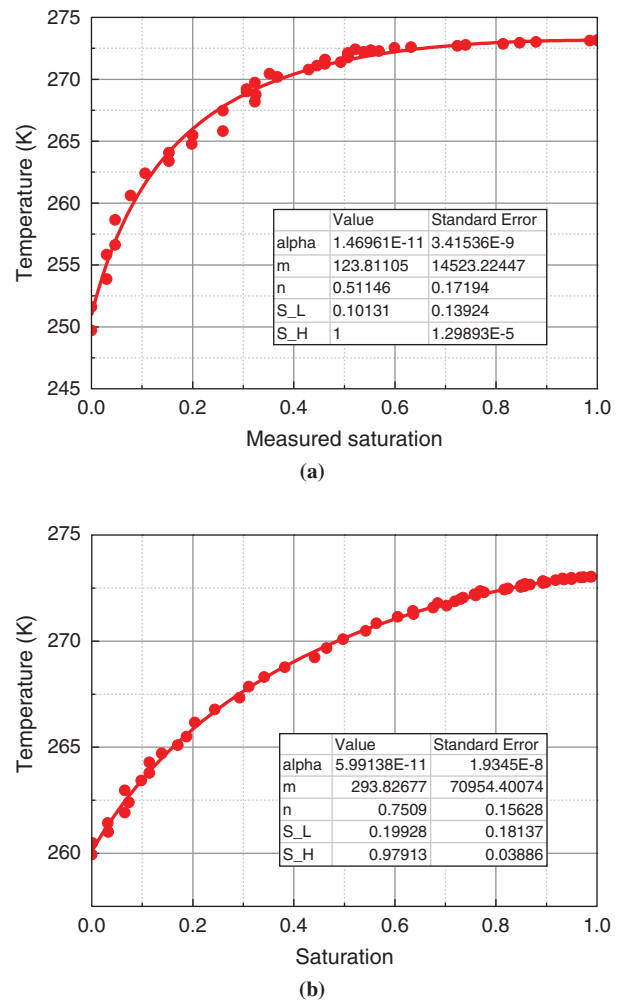
DISCUSSION OF RESULTS

Three questions need to be answered before the prediction equation can be confidently applied to various conditions:

1. Is this equation applicable to a variety of soils with significantly different properties?
2. Is this equation effective in a wide range of temperatures? That is, the good performance of the equation at relatively low temperatures (low saturations) needs to be proved.
3. Can this equation be applied in both freezing and thawing processes? In other words, can hysteresis be accommodated by this equation?

These questions are answered in this section by the application of the equation to analysis data reported by previous researchers. The measured saturations in the following graphs are normalized values according to Equation 20. This treatment does not harm the validity of the fitting results based on the discussion at the end of the section for the prediction equation.

The phase composition data reported by Anderson and Tice were used to investigate the applicability of the proposed equation in various soils and soil constituents (3). The reported curves cover five representative soils: Umiat bentonite, Hawaiian clay, Suffield silty clay, Dow Field silty clay, and basalt. As shown in Figure 5a, the prediction equation offers satisfactory curve fitting results for all of the five soils. For five representative soil constituents—kaolinite, powdered hematite, limonite, West Lebanon gravel, and Fairbanks

	Value	Standard Error
alpha	1.46961E-11	3.41536E-9
m	123.81105	14523.22447
n	0.51146	0.17194
S_L	0.10131	0.13924
S_H	1	1.29893E-5

(a)

	Value	Standard Error
alpha	5.99138E-11	1.9345E-8
m	293.82677	70954.40074
n	0.7509	0.15628
S_L	0.19928	0.18137
S_H	0.97913	0.03886

(b)

FIGURE 4 Comparisons between measured and fitted phase composition curves for (a) Soil 1 and (b) Soil 2.
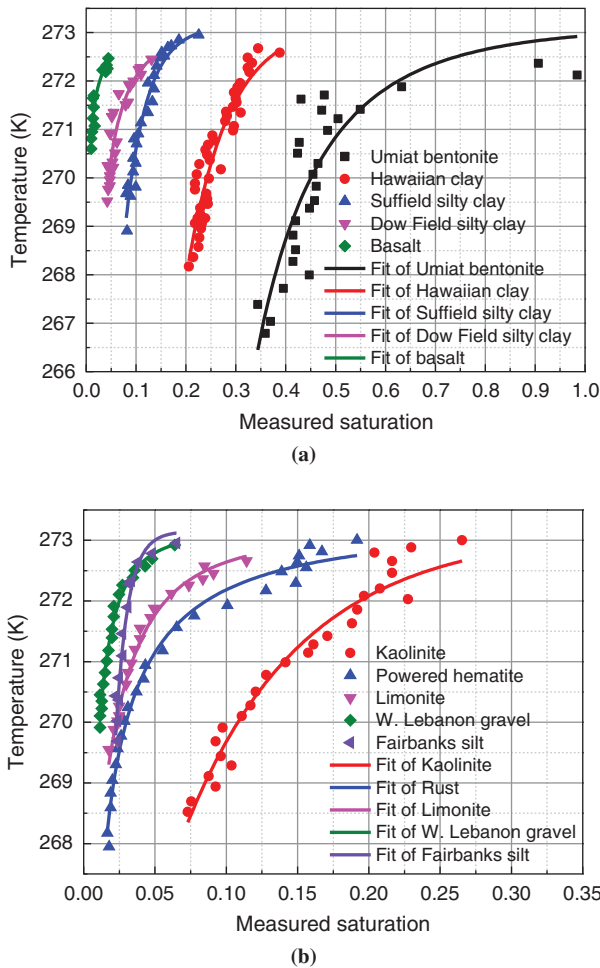
FIGURE 5   Measured and fitted phase composition curves for (*a*) five representative soils and (*b*) five representative constituents.

FIGURE 6   Measured and fitted phase composition curves for two soils over large temperature range.

silt—good comparisons between measured and fitted results were also obtained (Figure 5*b*). Therefore, it is safe to conclude that the prediction equation applies to various representative soils covering a wide range of soil properties.

Another concern for the prediction equation is its effectiveness in a large temperature range. To address this concern, the prediction equation was adapted to fit the phase composition curves measured by Yoshikawa and Overduin (*16*). The measured data were obtained by different sensors including TDR, nuclear magnetic resonance, frequency domain reflectometry (capacitance), and time domain transmissometry sensors. For this reason, the measured results cover a temperature range from the freezing point of bulk water to as low as 210 K. As shown in Figure 6, the measured data by different sensors appear to be scattered at low temperatures because of the difficulties in determining low unfrozen water content. For both a clay and the Fairbanks silt tested, the measured results are well fitted by the proposed prediction equation. Moreover, the divergence among measured data is compromised by the use of the prediction equation.

Similar to the soil water characteristic curve in unsaturated soils, the phase composition curves in the thawing and freezing processes of a single soil could be evidently different because of the influence of hysteresis. The hysteresis in the phase composition curve is attributed to two factors. One is related to contact angle, which
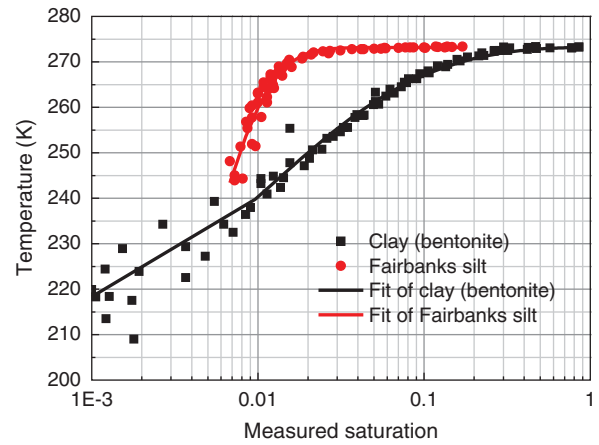
results from the irregularities of the internal structure and the difference between advancing and receding contact angles. Another factor includes the influences of entrapped air and thixotropic regain and aging effects, which contribute to variations of the pore size distribution. It is still questionable whether the proposed equation can be used to formulate the phase composition curves in both freezing and thawing processes. The phase composition curves for a colloidal soil in the freezing and thawing processes measured by Koopmans and Miller (*2*) were employed (*17*). As demonstrated in Figure 7, the proposed equation yields good fitting results for both processes. This finding indicates that the curve fitting for separate processes has considered the factors responsible for hysteresis by adjusting the fitting constants. Therefore, the prediction equation can be used to analyze both freezing and thawing processes and allow for the hysteresis between them.

CONCLUSION

A detailed physical basis for the phase composition curve in frozen soils was presented. The underlying physical mechanisms were discussed and the establishment of the phase composition curve based on these mechanisms was demonstrated step by step. On the basis
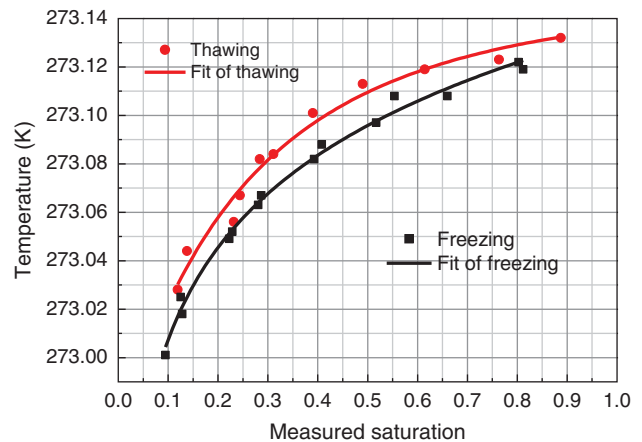

FIGURE 7   Measured and fitted phase composition curves for colloidal soil in freezing and thawing processes.

of the proposed physical basis, a prediction equation was proposed to take the place of the empirical equations used in previous studies. This physically based equation describes a unique relationship between saturation (unfrozen water content) and temperature. Information such as soil saturation under unfrozen conditions and the lowest temperature available in a test was considered. The equation has great flexibility in fitting different types of measured phase composition data that are in different units or expressed by different parameters. Experimental data measured by a thermo–TDR sensor were used to test the performance of the prediction equation. Excellent fitting results were obtained; these data verified the validity of the proposed equation. Additional calculations were conducted with data reported in previous studies. The applications of the equation in a variety of soils, in a large temperature range, and in both freezing and thawing processes were strongly supported by the good comparisons between measured and fitted results. Therefore, this study offers a solid physical basis and an effective prediction equation for the phase composition curve, both of which are lacking in previous studies. It is expected that the application of the phase composition curve will significantly benefit from this investigation.

REFERENCES

1. Williams, P. J. Unfrozen Water Content of Frozen Soils and Soil Moisture Suction. *Geotechnique,* Vol. 14, No. 2, 1964, pp. 133–142.
2. Koopmans, R. W. R., and R. D. Miller. Soil Freezing and Soil Water Characteristic Curves. *Soil Science Society of America Proceedings,* Vol. 30, No. 6, 1966, pp. 680–685.
3. Anderson, D. M., and A. R. Tice. Predicting Unfrozen Water Contents in Frozen Soils from Surface Area Measurements. In *Highway Research Record 393,* HRB, National Research Council, Washington, D.C., 1972, pp. 12–18.
4. Anderson, D. M., and N. R. Morgenstern. Physics, Chemistry and Mechanics of Frozen Ground: A Review. *Proc., 2nd International Conference on Permafrost,* Yakutsk, USSR, 1973, pp. 257–288.
5. Konrad, J.-M. Cold Region Engineering. In *Geotechnical and Geo-environmental Engineering Handbook* (R. K. Rowe, ed.), Kluwer Academic Publishers, Boston, Mass., 2001, pp. 591–613.
6. Konrad, J.-M. Sixteenth Canadian Geotechnical Colloquium: Frost Heave in Soils: Concepts and Engineering. *Canadian Geotechnical Journal,* Vol. 31, No. 2, 1994, pp. 223–245.
7. Dillon, H. B., and O. B. Andersland. Predicting Unfrozen Water Contents in Frozen Soils. *Canadian Geotechnical Journal,* Vol. 3, No. 2, 1966, pp. 53–60.
8. Spaans, E. J. A., and J. M. Baker. The Soil Freezing Characteristic: Its Measurement and Similarity to the Soil Moisture Characteristic. *Soil Science Society of America Journal,* Vol. 60, No. 1, 1996, pp. 13–19.
9. Liu, Z., X. Yu, Y. Sun, and B. Zhang. Formulation and Characterization of Freezing Saturated Soils. *Journal of Cold Regions Engineering,* Vol. 27, No. 2, 2012, pp. 94–107.
10. Tuller, M., D. Or, and L. M. Dudley. Adsorption and Capillary Condensation in Porous Media: Liquid Retention and Interfacial Configurations in Angular Pores. *Water Resources Research,* Vol. 35, No. 7, 1999, pp. 1949–1964.
11. Fredlund, D. G., and A. Xing. Equations for the Soil-Water Characteristic Curve. *Canadian Geotechnical Journal,* Vol. 31, No. 4, 1994, pp. 521–532.
12. Kay, B. D., and P. H. Groenevelt. On the Interaction of Water and Heat Transport in Frozen and Unfrozen Soils: I. Basic Theory: The Vapor Phase. *Soil Science Society of America Proceedings,* Vol. 38, No. 3, 1974, pp. 395–400.
13. Hansson, K. Water and Heat Transport in Road Structures: Development of Mechanical Models. In *Digital Comprehensive Summaries of Uppsala Dissertations,* Faculty of Science and Technology, Uppsala University, Sweden, 2005.
14. Mualem, Y. A New Model for Predicting the Hydraulic Conductivity of Unsaturated Porous Media. *Water Resources Research,* Vol. 12, No. 3, 1976, pp. 513–522.
15. van Genuchten, M. T. A Close-Form Equation for Predicting the Hydraulic Conductivity of Unsaturated Soil. *Soil Science Society of America Journal,* Vol. 44, No. 5, 1980, pp. 892–898.
16. Yoshikawa, K., and P. P. Overduin. Comparing Unfrozen Water Content Measurements of Frozen Soil Using Recently Developed Commercial Sensors. *Cold Regions Science and Technology,* Vol. 42, No. 3, 2005, pp. 250–256.
17. Miller, R. D. Soil Freezing in Relation to Pore Water Pressure and Temperature. *Proc., 2nd International Conference on Permafrost,* Yakutsk, USSR, 1973, pp. 257–288.